

**UCC Library and UCC researchers have made this item openly available.  
 Please [let us know](#) how this has helped you. Thanks!**

<b>Title</b>	Multimodal behavior of the dynamic magnetic susceptibility spectrum in amorphous CoZrTaB magnetic thin films
<b>Author(s)</b>	Jordan, Declan; Wei, Guannan; Masood, A.; O'Mathuna, Cian; McCloskey, Paul
<b>Publication date</b>	2020-09-02
<b>Original citation</b>	Jordan, D., Wei, G., Masood, A., O'Mathuna, C. and McCloskey, P. (2020) 'Multimodal behavior of the dynamic magnetic susceptibility spectrum in amorphous CoZrTaB magnetic thin films', Journal of Applied Physics, 128, 093902 (8pp). doi: 10.1063/5.0013962
<b>Type of publication</b>	Article (peer-reviewed)
<b>Link to publisher's version</b>	<a href="http://dx.doi.org/10.1063/5.0013962">http://dx.doi.org/10.1063/5.0013962</a> Access to the full text of the published version may require a subscription.
<b>Rights</b>	© 2020, the Authors. All article content, except where otherwise noted, is licensed under a Creative Commons Attribution (CC BY) license ( <a href="http://creativecommons.org/licenses/by/4.0/">http://creativecommons.org/licenses/by/4.0/</a> ) <a href="https://creativecommons.org/licenses/by/4.0/">https://creativecommons.org/licenses/by/4.0/</a>
<b>Item downloaded from</b>	<a href="http://hdl.handle.net/10468/12224">http://hdl.handle.net/10468/12224</a>

Downloaded on 2021-11-27T17:10:25Z

# Multimodal behavior of the dynamic magnetic susceptibility spectrum in amorphous CoZrTaB magnetic thin films

Cite as: J. Appl. Phys. **128**, 093902 (2020); <https://doi.org/10.1063/5.0013962>

Submitted: 15 May 2020 • Accepted: 20 August 2020 • Published Online: 02 September 2020

 D. Jordan, G. Wei, A. Masood, et al.



View Online



Export Citation



CrossMark

## ARTICLES YOU MAY BE INTERESTED IN

[Soft magnetic nanocomposite CoZrTaB-SiO<sub>2</sub> thin films for high-frequency applications](#)

Journal of Applied Physics **127**, 243903 (2020); <https://doi.org/10.1063/5.0013416>

[FORC signatures and switching-field distributions of dipolar coupled nanowire-based hysterons](#)

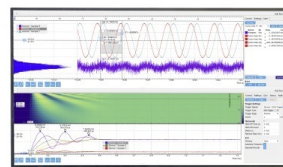
Journal of Applied Physics **128**, 093903 (2020); <https://doi.org/10.1063/5.0020407>

[Evolution of superparamagnetism in the electrochemical dealloying process](#)

Journal of Applied Physics **128**, 093904 (2020); <https://doi.org/10.1063/5.0015397>

Challenge us.

What are your needs for periodic signal detection?



Zurich  
Instruments



# Multimodal behavior of the dynamic magnetic susceptibility spectrum in amorphous CoZrTaB magnetic thin films

Cite as: J. Appl. Phys. 128, 093902 (2020); doi: 10.1063/5.0013962

Submitted: 15 May 2020 · Accepted: 20 August 2020 ·

Published Online: 2 September 2020



D. Jordan,<sup>1,a)</sup> G. Wei,<sup>1</sup> A. Masood,<sup>1</sup> C. O'Mathuna,<sup>1,2</sup> and P. McCloskey<sup>1</sup>

## AFFILIATIONS

<sup>1</sup>Tyndall National Institute, University College Cork (UCC), Lee Maltings, Dyke Parade, Cork T12 R5CP, Ireland

<sup>2</sup>School of Engineering, University College Cork (UCC), College Road, Cork T12 YN60, Ireland

<sup>a)</sup>Author to whom correspondence should be addressed: [declan.jordan@tyndall.ie](mailto:declan.jordan@tyndall.ie)

## ABSTRACT

The origins of sub-Ferromagnetic Resonance (FMR) multimodal behavior in the magnetic susceptibility spectrum of amorphous CoZrTaB magnetic thin films are investigated using Brown's diffusion model describing continuous diffusion of magnetic spins. Brown's diffusion model is regressed onto experimental data for the amorphous CoZrTaB magnetic thin films with thicknesses spanning 80–530 nm. The mathematical model presented successfully reproduces the thickness dependent dynamic magnetic susceptibility of the amorphous CoZrTaB magnetic thin films with strong statistical significance. The model proposes the formation of additional energy wells in the uniaxial anisotropy energy plane of the material after a critical film thickness. The sub-FMR resonance peaks arise when the frequency of the external excitation field approaches the natural frequency of the well. Furthermore, the additional energy wells in the anisotropy energy plane cause a breakdown in the axial symmetry of the anisotropy energy plane. This breakdown of axial symmetry results in dynamic coupling between the transverse ( $\chi_{\perp}$ ) and longitudinal ( $\chi_{\parallel}$ ) magnetic susceptibility. This dynamic coupling results in the initial low frequency step-down in the magnetic susceptibility observed in the thicker CoZrTaB magnetic thin films. It is found that the application of an external bias magnetic field along the easy axis of the amorphous CoZrTaB magnetic thin films suppresses the sub-FMR resonance peaks by restoring the axial symmetry of the anisotropy energy plane.

© 2020 Author(s). All article content, except where otherwise noted, is licensed under a Creative Commons Attribution (CC BY) license (<http://creativecommons.org/licenses/by/4.0/>). <https://doi.org/10.1063/5.0013962>

## I. INTRODUCTION

The dynamic magnetic susceptibility spectrum of CoZrTaB magnetic thin films has been extensively studied for more than a decade as it plays a critical role in the materials' performance in applications ranging from magnetic recordings and data storage,<sup>1</sup> to the magnetic passive component used in high frequency DC–DC converters.<sup>2</sup> It has been well reported in the literature that soft thin film magnetics used as the magnetic passive in DC–DC converters greatly increases the energy density of the converter while maintaining high efficiencies at very high frequencies.<sup>3</sup> The frequency loss characteristic of the magnetic material used in DC–DC converters is especially important as the miniaturization trend for power electronics is driven by the increased operating frequency of the DC–DC converter. The increased operating frequency of the converter enables a reduction in the physical size of the magnetic

passive component. Thus, the ability of soft magnetic CoZrTaB thin films to retain in-plane uniaxial anisotropy is important in order to ensure a low loss tangent ( $\chi''/\chi'$ ) at frequencies spanning 1–300 MHz. The frequency dependent loss tangent is fundamentally determined by the internal anisotropy energy plane<sup>4</sup> as it governs the magnetization dynamics of the material.<sup>5</sup> Ultra-low loss performance in the 1–300 MHz frequency range is achieved by having a material whose dynamic magnetic susceptibility is governed by transverse magnetic susceptibility ( $\chi_{\perp}$ ), with a single Ferromagnetic Resonance (FMR) peak in the GHz frequency range. This is typically achieved by materials with a strong in-plane uniaxial anisotropy energy plane. For such materials, the internal anisotropy energy plane is determined by one state variable, namely, the colatitude ( $\vartheta$ ) state variable.<sup>6</sup> Materials with a strong in-plane uniaxial anisotropy have a low loss tangent as the imaginary component of the

transverse magnetic susceptibility ( $\chi''_{\perp}$ ) is exceedingly small up until the onset of ferromagnetic resonance.

However, above a critical film thickness shape effects can break the axial symmetry of the internal anisotropy energy plane of the material. This results in the internal anisotropy energy plane being governed by two state variables, namely, the colatitude ( $\theta$ ) and azimuthal ( $\varphi$ ) state variables.<sup>6</sup> As a consequence of the thickness dependent axial symmetry of the anisotropy energy plane, there is a deterioration in the soft magnetic properties<sup>7</sup> and a growing proportion of magnetic spins whose preferred orientation is out of plane<sup>8–10</sup> with increasing film thickness. Moreover, the dependence of the internal anisotropy energy plane on two state variables results in dynamic coupling between the transverse magnetic susceptibility ( $\chi_{\perp}$ ) and the longitudinal magnetic susceptibility ( $\chi_{\parallel}$ ).<sup>11</sup> This dynamic coupling is further detrimental to the high frequency performance of the magnetic material as there is a rise in the low frequency imaginary component of the magnetic susceptibility caused by the presence of  $\chi''_{\parallel}$ . The coupling of the transverse and longitudinal magnetic susceptibilities limits the effective useful thickness of the CoZrTaB film. The onset of this coupling effect was observed between 220 and 333 nm for our  $3 \times 3 \text{ mm}^2$  samples.

Furthermore, multiple energy wells, each with a local minima, in the anisotropy energy plane could be used to explain the existence of the multiple sub FMR resonance peaks observed in the magnetic susceptibility spectrum reported in amorphous CoZrTaB (this work), CoNbZr,<sup>12</sup> and CoFeSiB,<sup>13</sup> magnetic thin films. The resonance frequencies are determined by the gradient of the anisotropy energy well and the amplitude of the resonance peaks determined by the depth of the anisotropy energy well. Hence, shallower energy well spins have smaller resonance peaks, which occur at lower frequencies. The application of an external magnetic field applied to the thin film can alter the gradient of the internal anisotropy energy by raising and/or lowering the barrier heights separating the energy wells.<sup>14</sup> Thus, the multiple sub-FMR resonance peaks can be suppressed through the application of an external biasing field. In this work, Brown's continuous diffusion model<sup>15</sup> is used to characterize the multimodal behavior in the magnetic susceptibility spectrum of the amorphous CoZrTaB magnetic thin films.

The structure of the paper is as follows: Sec. I provides an overview of multimodal behavior observed in amorphous magnetic thin films; Sec. II outlines the fabrication methods and experimental characterizations of the amorphous CoZrTaB magnetic thin films; Sec. III describes Brown's continuous diffusion model<sup>15</sup> used to characterize the magnetic susceptibility spectrum of the amorphous CoZrTaB magnetic thin films; Results and discussions are provided in Sec. IV; and finally conclusions of the paper are presented in Sec. V.

## II. EXPERIMENTAL METHODS AND MEASUREMENTS

Amorphous  $\text{Co}_{84}\text{Zr}_4\text{Ta}_4\text{B}_8$  magnetic thin films spanning thicknesses 80–530 nm were magnetron sputter deposited at 500 W DC in the presence of an aligning magnetic field.<sup>16</sup> The sputtering chamber was evacuated until a pressure of  $10^{-6}$  Pa was measure, after which Argon gas was pumped into the chamber until a sputter pressure of 0.13 Pa was achieved. The film thicknesses were measured using a DekTak surface profilometer. The atomic composition and the amorphous structure of the films were confirmed

using x-ray diffraction (Phillips Xpert diffractometer) and transmission electron microscopy. The dynamic magnetic susceptibility of the films was measured from 1 MHz to 9 GHz using a small signal wideband complex permeameter (Ryowa Electronics, Japan, Model PMM 9G) on the  $3 \times 3 \text{ mm}^2$  samples. Note that the dimensions of the samples were constant for all thickness, i.e., all samples were  $3 \times 3 \text{ mm}^2$ . The results of the atomic composition and material morphology are discussed in Ref. 16.

## III. N MINIMA ANISOTROPY MODEL

The dynamic magnetic susceptibility of amorphous magnetic materials subject to a weak AC driving field can be determined using linear response theory,<sup>17</sup>

$$\mathbf{M} = \chi \mathbf{H}. \quad (1)$$

Here,  $\mathbf{M}$  is the magnetization vector of the thin film;  $\mathbf{H}$  is the magnetic field acting on the thin film; and  $\chi$  is the dynamic magnetic susceptibility of the thin film. The dynamic magnetic susceptibility of the thin film subject to an external driving field can be expressed as a weighted sum of longitudinal and transverse magnetic susceptibilities. This weighted combination is expressed in Eq. (2),

$$\chi(\omega) = \chi_{\parallel}(0)\chi_{\parallel}(\omega) + \chi_{\perp}(0)\chi_{\perp}(\omega). \quad (2)$$

Here,  $\chi_{\parallel}(0)$  and  $\chi_{\perp}(0)$  are the static longitudinal and transverse magnetic response. The  $\chi_{\parallel}(0)$  and  $\chi_{\perp}(0)$  coefficients are determined by the internal anisotropy energy plane of the thin film. The longitudinal component of the magnetic susceptibility can be modeled using the two mode approximation<sup>18</sup> [see Eq. (3)],

$$\chi_{\parallel}(\omega) = \chi_{\parallel}(0) \left( \frac{\Delta_1}{1 + i\omega\tau} + \frac{1 - \Delta_1}{1 + i\omega\tau_w} \right). \quad (3)$$

Here,  $\Delta_1$  and  $\tau_w$  are parameters determined to ensure correct behavior of  $\chi_{\parallel}(\omega)$  at the very low frequency and very high frequency extremes. The transverse magnetic susceptibility response for strong in-plane uniaxial anisotropy can be determined from the Landau–Lifshitz equation<sup>19</sup> [see Eq. (4)],

$$\chi_{\perp}(\omega) = \chi_{\perp}(0) \frac{(1 + \alpha^2)\omega_{pr}^2 + i\alpha\omega\omega_{pr}}{(1 + \alpha^2)\omega_{pr}^2 - \omega^2 + i2\alpha\omega\omega_{pr}}. \quad (4)$$

Here,  $\omega_{pr}$  is the natural precession frequency of the magnetic moments of the thin and  $\alpha$  is a viscous damping parameter acting on the magnetic moments. This frequency is determined by the internal gradient of the anisotropy energy plane. Note any vector *field* can be expressed as the gradient of a scalar potential. Hence, the precession frequency is governed by the anisotropy field ( $\mathbf{H}_{an}$ ) and gradient of the anisotropy energy plane of the thin film ( $\nabla_M V$ ). This relationship between the precession frequency, the anisotropy field, and the anisotropy energy plane is explicitly stated in Eqs. (5) and (6). Thus, the shape of the anisotropy energy plane is of critical importance to the precession frequency. Typically, materials with strong in-plane uniaxial anisotropy are characterized by two distinct energy wells separated by a barrier. Thus, each well has its own

precession frequency determined by the shape of the well,

$$\omega_{pr} \approx \gamma H_{an} = -\gamma \nabla_M V, \tag{5}$$

$$H_{an} = \sqrt{H_{KP}(H_{KP} + 4\pi M_s)}. \tag{6}$$

Note that Eq. (6) relates the *in-plane uniaxial anisotropy* field ( $H_{KP}$ ) to the *anisotropy* field. Ferromagnetic resonance occurs when the frequency of the driving field approaches the precession frequency of the well. For a symmetric two well structure, the precession frequencies of both wells are identical and so only a single FMR peak is observed at  $\omega \rightarrow \omega_{pr}$ . The amplitude and quality

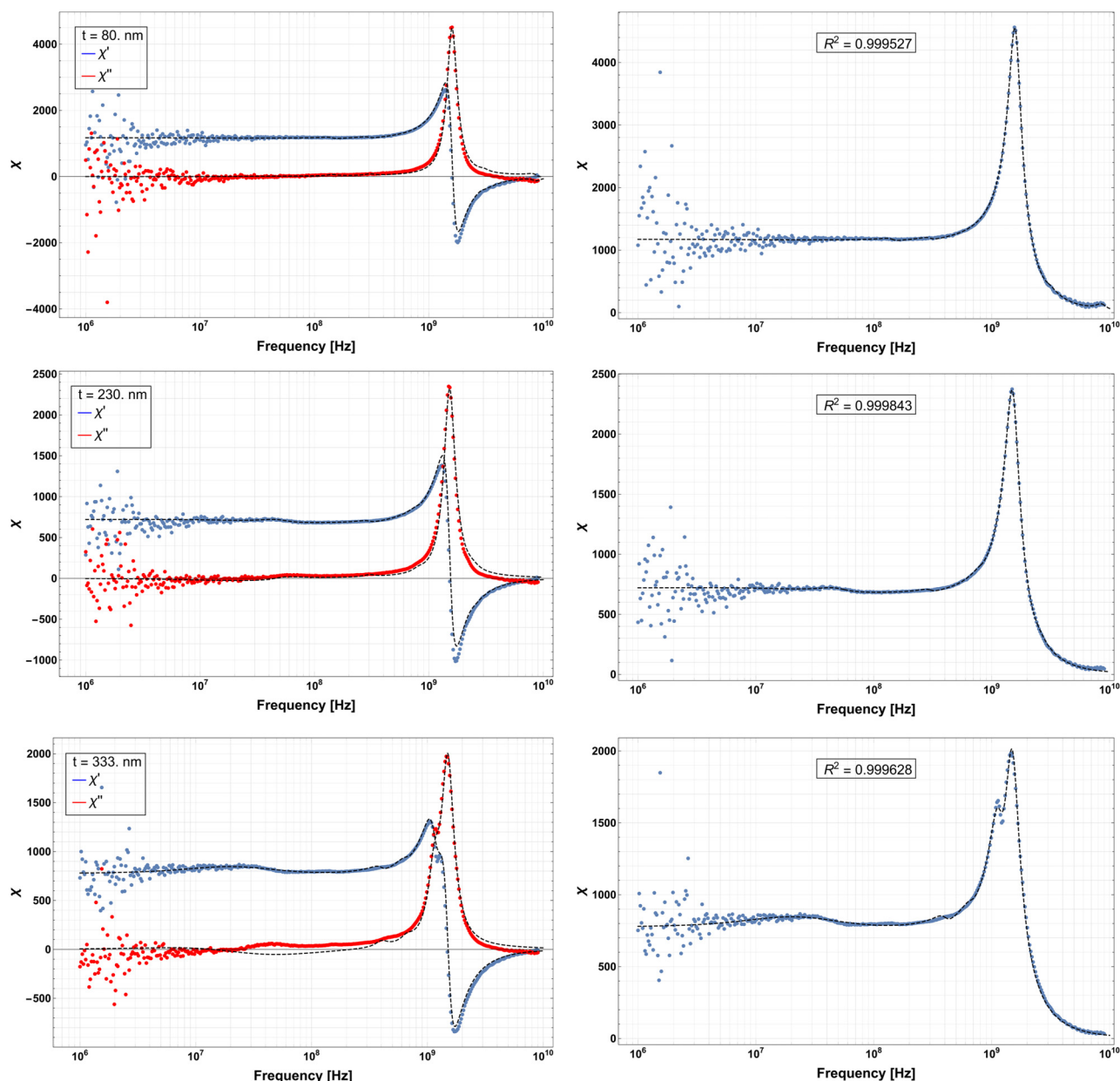


FIG. 1. Magnetic susceptibility data for amorphous CoZrTaB magnetic thin films spanning thickness 80–530 nm. (Left) Real and imaginary magnetic susceptibility. (Right) Absolute magnetic susceptibility. Dashed lines are the fitted model.

factor of the FMR peak is determined by the shape and depth of the well, along with the viscous damping acting on precession of the magnetic moments. Here, the quality factor of the FMR peak refers to the ratio of peak's amplitude to width. Reduction in the barrier height separating the two energy wells causes a dispersion of the precession frequency and results in reduced quality of the FMR peak. That is, the FMR peak becomes smaller and wider.

Equation (4) accurately predicts a single FMR peak for materials with in-plane uniaxial anisotropy as both energy wells are identical and there is only a single precession frequency. Therefore, Eq. (4) must be modified to account for the multiple sub-FMR peaks observed in the thicker magnetic films. The *Ansatz* or assumption of this work is that each sub-FMR peak observed in the magnetic films has a corresponding energy well with a distinct precession frequency. Therefore, each distinct energy well will exhibit resonance behavior as the excitation frequency of the applied external magnetic field approaches the precession frequency of the energy well. This is shown in Eq. (7),

$$\chi_{\perp}(\omega) = \chi_{\perp}(0) \sum_{k=1}^N c_k \frac{(1 + \alpha^2)\omega_{pr,k}^2 + i\alpha\omega\omega_{pr,k}}{(1 + \alpha^2)\omega_{pr,k}^2 - \omega^2 + i2\alpha\omega\omega_{pr,k}}. \quad (7)$$

Here,  $\omega_{pr,k}$  and  $c_k$  denote the precession frequency and depth of the  $k$ th energy well. In the case of uniaxial anisotropy, Eq. (7) reduces to Eq. (4) with  $c_1 = 1$  and the remaining  $c_k = 0$ .

#### IV. RESULTS AND DISCUSSION

Nonlinear model fitting is used to regress Eqs. (2), (3), and (7) onto the frequency dependent magnetic susceptibility of the 80–530 nm films. The results of the regression are presented in Fig. 1. The N Minima model accurately fits to the thickness dependent multimodal behavior of the dynamic magnetic susceptibility of the films with an R-squared value of 0.99, as illustrated in Fig. 1. The R-squared value of 0.99 indicates that the model fits the data with a strong statistical significance. Hence, the *Ansatz* that the anisotropy energy plane of the thicker films is best described as in-plane uniaxial degraded by superfluous energy wells is justified. Thus, the shape of the internal anisotropy energy plane can be inferred by regressing the model onto the dynamic magnetic susceptibility of the thin films.

More importantly, the frequency position of the multiple FMR peaks did not change with increasing film thickness, rather the amplitude of the peaks was increased. The frequency position of the FMR peak is ultimately determined by the gradient of the energy well. Therefore, the depths of the energy wells [represented

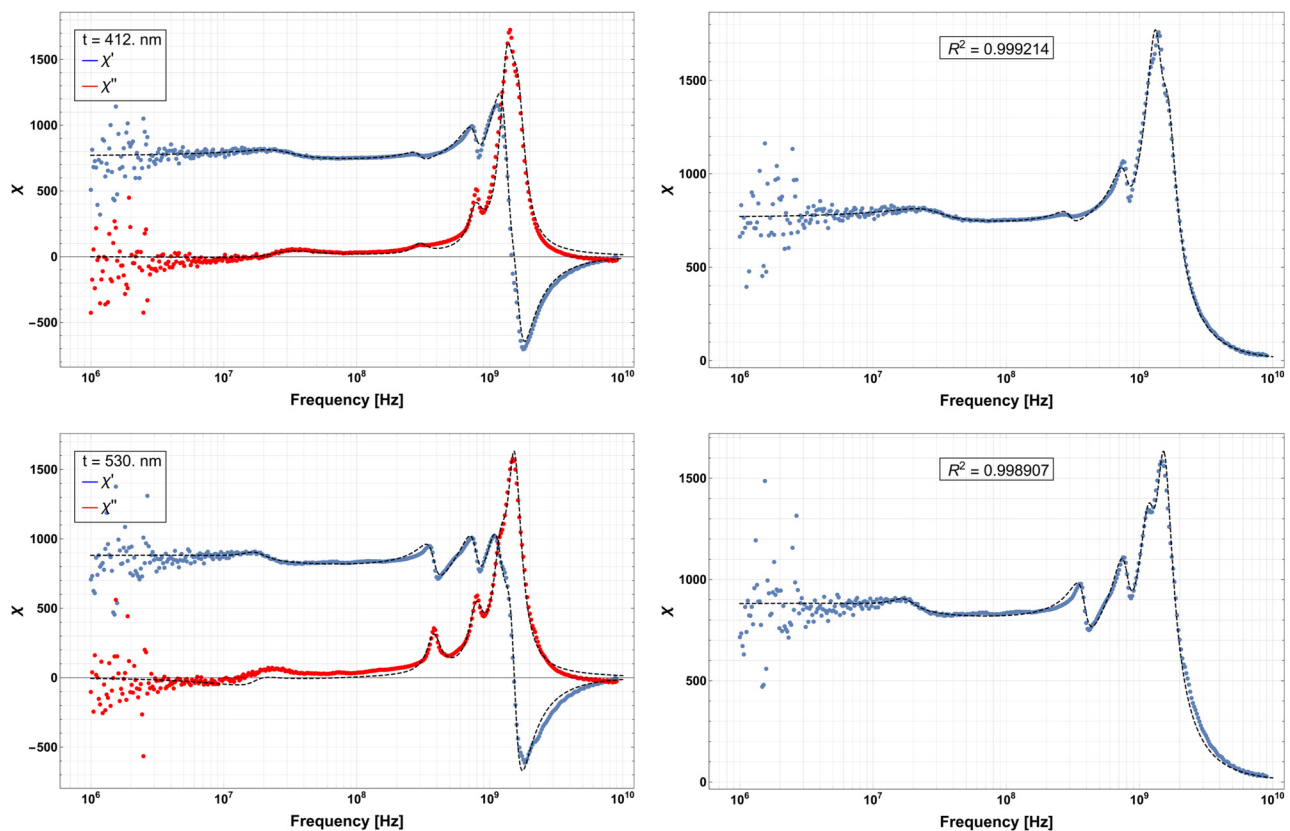
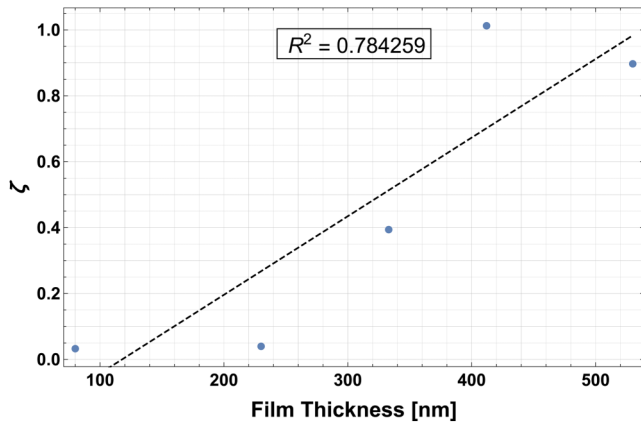
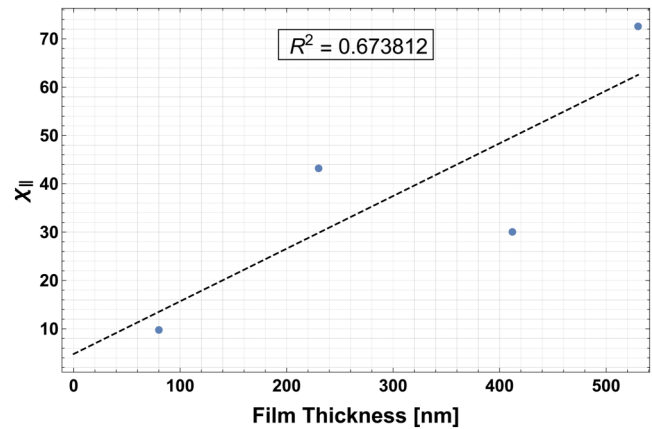


FIG. 1. (Continued.)



**FIG. 2.** The ratio of the sum of the  $c_k$  coefficients (for  $k>1$ ) to uniaxial anisotropy coefficient ( $c_1$ ) determined by regressing Eq. (7) onto the experimental magnetic susceptibility of the amorphous CoZrTaB magnetic thin films (see Fig. 1).



**FIG. 3.** Amplitude of the longitudinal magnetic susceptibility in thin films vs film thickness. (Note that the 333 nm thick CoZrTaB magnetic thin film is omitted from this plot as the low frequency noise on the magnetic susceptibility measurement resulted in a lower  $\chi_{||}$ . The effect of the noise is also seen as an error in the modeled low frequency imaginary component of the magnetic susceptibility of the film.)

by the  $c_k$  coefficients in Eq. (7)] increased without changing the gradient of the well. An observed shift in the frequency position of the resonance peak would indicate a change in the shape of the energy well. The observed reduction in the amplitude and quality factor of the primary FMR peak is caused by a decrease in the barrier height of the primary well. This reduction in the primary FMR peak is known as inhomogeneous broadening<sup>20,21</sup> and is observed in the dynamic magnetic susceptibility of the amorphous CoZrTaB magnetic thin films (see Fig. 1). This is consistent with the depth of the well determining the quality of the resonance peaks through inhomogeneous broadening as the resonance peak will still be centered on the primary precession frequency of the well, even in the event of dispersion of the precession frequency through inhomogeneous broadening. Hence, the amplitude and frequency position of the peaks could be used to draw inference on the underlying physical phenomena causing the existence of the energy wells.

The reduction in the quality factor (ratio of amplitude to width) of the primary resonance peak in the thicker films (see Fig. 1) is a consequence of the reduction in the barrier height of the uniaxial anisotropy energy well due to the emergence of the mixed anisotropy. For a small to moderate barrier height ( $1 \leq \sigma \leq 5$ ), there is essentially a dispersion of the precession frequencies of the magnetization within the anisotropy well. This effect presents itself as inhomogeneous broadening of the primary FMR peak as the effect considerably exceeds the actual damping parameter ( $\alpha$ ) of the material.<sup>20,21</sup>

Figure 2 shows the ratio of  $c_k$  coefficients in Eq. (7) to uniaxial anisotropy plotted for the various films presented in Fig. 1. It is evident that as the amorphous CoZrTaB films become thicker, the anisotropy energy plane is more heavily influenced by additional energy wells

within the anisotropy field. This is shown as there is a near linear relationship between increasing film thickness and the amplitude of the  $c_k$  coefficients representing the depths of the energy wells. From this graph, we can conclude that there is a reduction in the barrier height of the in-plane anisotropy caused by the formation of superfluous energy wells with increasing film thickness. The reduction in the amplitude of the anisotropy field is later verified in Fig. 4. Importantly, the additional energy wells in the anisotropy energy plane result in a breakdown of the axial symmetry of the anisotropy energy plane. This results in dynamic coupling between the longitudinal and transverse magnetic susceptibilities of the thicker films. Hence, there will be an observed increase in  $\chi_{||}$  with increasing film thickness.

The amplitude of  $\chi_{||}$  vs film thickness is shown in Fig. 3. The increase in the longitudinal magnetic susceptibility is responsible for the initial low frequency drop-off in the magnetic susceptibility of the films. This drop-off occurs between 10 and 100 MHz (see Fig. 1). The low frequency drop in magnetic susceptibility is incredibly detrimental to the performance of the magnetic thin film used in DC-DC power converters. The initial drop is caused by a growth in the imaginary component of the longitudinal magnetic susceptibility and results in a higher loss tangent at lower frequencies.

The breakdown in the uniaxial anisotropy results in greater degrees of freedom in the magnetization dynamics as the evolution equation for the magnetic thin film is no longer governed by a single state variable. Instead, it is governed by two state variables. The magnetization dynamics of a thin film with two state variables is governed by the Fokker-Planck equation<sup>15,22</sup> [Eq. (8)],

$$\frac{\partial W}{\partial t} = k\Delta W + \frac{h'}{\sin \vartheta} \left\{ \frac{\partial}{\partial \vartheta} \left[ \left( \sin \vartheta \frac{\partial V_{\vartheta, \varphi}}{\partial \vartheta} + \frac{\partial V_{\vartheta, \varphi}}{\alpha \partial \varphi} \right) W \right] + \frac{\partial}{\partial \varphi} \left[ \left( \frac{1}{\sin \vartheta} \frac{\partial V_{\vartheta, \varphi}}{\partial \varphi} - \frac{\partial V_{\vartheta, \varphi}}{\partial \vartheta} \right) W \right] \right\}. \quad (8)$$

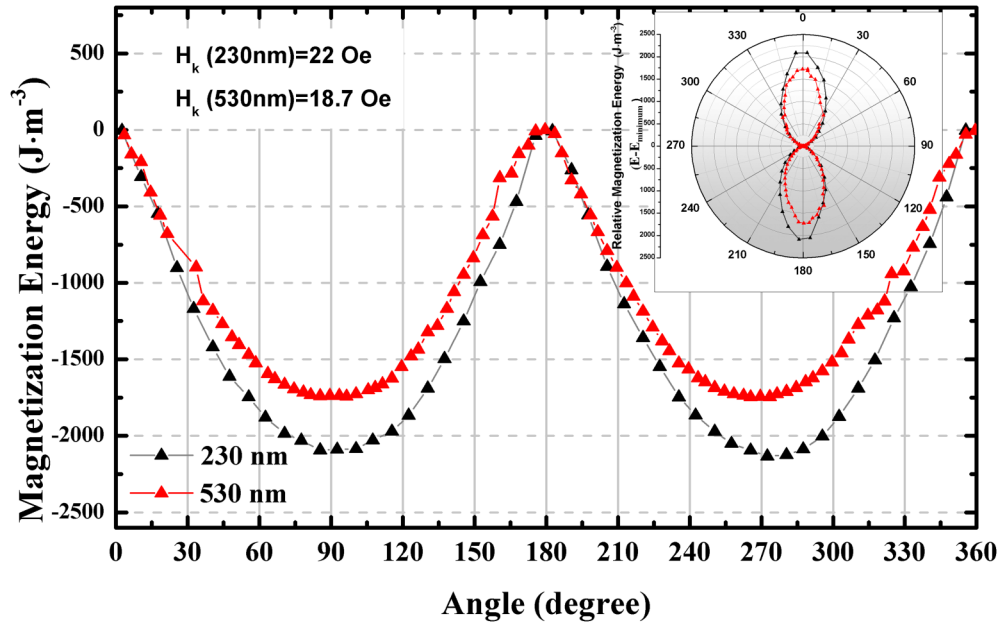


FIG. 4. In-plane anisotropy of 230 nm and 530 nm amorphous CoZrTaB magnetic thin films (polar plot inset).

Here,  $h'$  is Brown's parameter, which relates the damping and gyro-magnetic moment to the magnetization saturation;  $V_{\theta, \varphi}$  is the sum of all the internal anisotropies; and  $W$  is the probability distribution function that a magnetic moments orientation lies within an infinitesimally small segment of the unit sphere. Note that  $k$  is determined by requiring the steady state distribution of Eq. (8) to be Boltzmann,

$$h' = \frac{\alpha\gamma}{(1 + \alpha^2)M_s}, \quad (9)$$

$$k = \frac{K_B T h'}{\nu}. \quad (10)$$

For uniaxial anisotropy, the energy term is governed by Eq. (11),

$$V_{\theta} = K \sin^2\theta. \quad (11)$$

Hence, for uniaxial anisotropy, the  $\frac{\partial}{\partial \varphi}$  term in Eq. (8) drops out. Therefore, for uniaxial anisotropy, there is no dynamic coupling between the transverse and longitudinal components of the

magnetization dynamics. However, for more complex anisotropies with an azimuthal dependence, there will be dynamic coupling between the transverse and longitudinal components of the magnetization dynamics—resulting in higher material loss.

The magnetization energy band of the 230 nm and 530 nm films is presented in Fig. 4. There is a notable reduction in the amplitude of the anisotropy field within the thicker film. This is consistent with the observed inhomogeneous broadening of the primary FMR peak (shown in Fig. 1) caused by the reduction in the barrier height of the in-plane anisotropy energy well (shown in Fig. 2). Furthermore, Fig. 4 shows clear deviations from in-plane uniaxial anisotropy in the 530 nm film caused by additional energy wells with local energy minima. The existence of the additional energy wells in the anisotropy energy plane causes the multimodal behavior of the dynamic magnetic susceptibility observed in the thicker films. Furthermore, the presence of the additional energy wells also explains the dynamic coupling between the longitudinal and transverse magnetic susceptibility observed in the thicker films. For clarity, the positions of the additional energy minima observed in the 530 nm thick film are presented in Table I.

The internal anisotropy of the material can be biased through the application of a DC external field.<sup>23–25</sup> When applied at an

TABLE I. Angular positions of energy minima for 530 nm amorphous CoZrTaB magnetic thin film shown in Fig. 4.

	Well 1	Well 2	Well 3	Well 4
Angular position of well ( $\theta$ )	10°	25° ≤ $\theta$ ≤ 35°	160° ≤ $\theta$ ≤ 165°	310° ≤ $\theta$ ≤ 330°



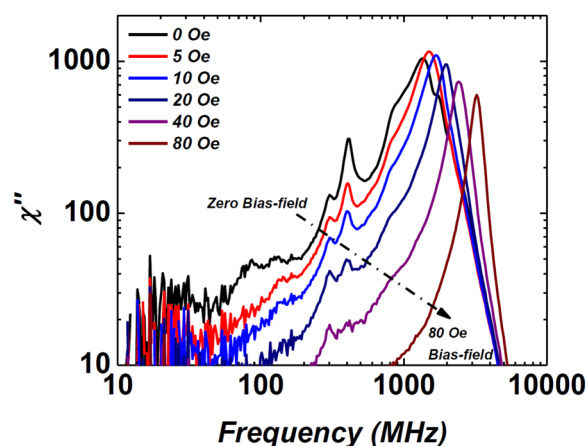


**FIG. 5.** Magnetic susceptibility of 530 nm amorphous CoZrTaB magnetic thin film subjected to DC bias field applied along the easy axis.

oblique angle to the easy axis, the bias field breaks the axial symmetry of the anisotropy energy plane. However, applying a DC bias field along the easy axis of the thin film can alter the internal anisotropy energy plane while maintaining axial symmetry. This is important as non-axial symmetry of the anisotropy energy plane causes dynamic coupling between the longitudinal and transverse dynamic magnetic susceptibility. The effect of the DC bias field along the easy axis is shown in Fig. 5. Note in Fig. 5 that the amplitudes of the multiple resonance peaks are diminished with increasing amplitude of the DC bias field. From the regressed model, this suggests that the applied DC bias field smoothens out the additional energy minima in the internal anisotropy energy plane. Furthermore, the shift in the FMR peak toward higher frequencies is again accounted for by the increased gradient of the internal anisotropy energy plane caused by the biasing field.

Hence, a DC bias field may be used to counter the effect of the thickness dependent multimodal behavior in the magnetic susceptibility spectrum of amorphous CoZrTaB magnetic thin films via the restoration of uniaxial anisotropy within the film. This is important for DC-DC power converters that utilize amorphous CoZrTaB magnetic thin films (or other materials that exhibit the multimodal behavior) as the DC bias field can be used to tune the loss within the amorphous thin film and allow for thicker layers of amorphous thin films to be used in the converters.

Moreover, the use of micro-patterning can alter the internal anisotropy energy plane through shape demagnetization. Therefore, micro-patterning of the amorphous CoZrTaB magnetic thin films can be used to suppress the multimodal behavior of the dynamic magnetic susceptibility. Indeed, such micro-patterning was successfully used by Yamaguchi *et al.*<sup>26</sup> to improve the high frequency performance of amorphous CoNbZr magnetic thin films (CoNbZr also exhibits multimodal behavior). It is clear from the inductance plot<sup>26</sup> that micro-patterning of the thin film along the easy axis stymies the formation of sub-FMR resonance peaks by altering the shape anisotropy.

## V. CONCLUSIONS

We have treated the problem of multimodal behavior in the magnetic susceptibility spectrum of amorphous CoZrTaB magnetic thin films spanning 80–530 nm thickness using Brown's continuous diffusion model of magnetic spins. The model was regressed onto the experimental data and achieved R-squared values above 0.99. The model reproduced the dynamic magnetic susceptibility of the amorphous CoZrTaB magnetic thin films with strong statistical significance. The observed sub-FMR multimodal behavior in the dynamic magnetic susceptibility is attributed to the formation of additional energy wells in the uniaxial anisotropy energy plane of the thin films. We have shown how the breakdown in the uniaxial anisotropy of the thin films results in dynamic coupling between the transverse ( $\chi_{\perp}$ ) and longitudinal ( $\chi_{\parallel}$ ) magnetic susceptibility. The main tractability of this model is that inference can be made to the shape of the internal anisotropy energy plane by regressing the model onto the measured dynamic magnetic susceptibility of the material. From this inference, structural properties of the material can be indirectly determined.

Furthermore, the reduction in the main barrier height of the uniaxial anisotropy causes a dispersion of the primary precession frequency resulting in the inhomogeneous broadening of the primary FMR peak. We have also shown how the application of an external bias field can be used to diminish the energy minima of the anisotropy field suppressing the multimodal behavior of the magnetic susceptibility.

## ACKNOWLEDGMENTS

The authors would like to acknowledge the EU GaNonCMOS Project (No. EU-H2020-NMBP-2016-721107) and the SFI ADEPT Project (No. 15/IA/3180).

## DATA AVAILABILITY

The data that support the findings of this study are available from the corresponding author upon reasonable request.

## REFERENCES

- 1K. Tanahashi, A. Kikukawa, and Y. Hosoe, "Exchange-biased CoTaZr soft underlayer for perpendicular recording," *J. Appl. Phys.* **93**(10), 8161–8163 (2003).
- 2C. Ó. Mathúna, N. Wang, S. Kulkarni, and S. Roy, "Review of integrated magnetics for power supply on chip (PwrSoC)," *IEEE Trans. Power Electron.* **27**(11), 4799–4816 (2012).
- 3D. V. Harburg *et al.*, "Microfabricated racetrack inductors with thin-film magnetic cores for on-chip power conversion," *IEEE J. Emerg. Sel. Topics Power Electron.* **6**(3), 1280–1294 (2018).
- 4J. M. Coey, *Magnetism and Magnetic Materials* (Cambridge University Press, 2010), pp. 9–12.
- 5H. C. Siegmann and J. Stöhr, *Magnetism: From Fundamentals to Nanoscale Dynamics* (Springer, 2006).
- 6Y. P. Kalmykov, W. T. Coffey, B. Ouari, and S. V. Titov, "Damping dependence of the magnetization relaxation time of single-domain ferromagnetic particles," *J. Magn. Magn. Mater.* **292**, 372–384 (2005).
- 7A. Masood and P. McCloskey, C. Ó. Mathúna, and S. Kulkarni, "Controlling the competing magnetic anisotropy energies in FineMET amorphous thin films with ultra-soft magnetic properties," *AIP Adv.* **7**(5), 055208 (2017).

- <sup>8</sup>P. Sharma, H. Kimura, and A. Inoue, "Magnetic behavior of cosputtered Fe-Zr amorphous thin films exhibiting perpendicular magnetic anisotropy," *Phys. Rev. B* **78**(13), 134414 (2008).
- <sup>9</sup>P. Sharma, H. Kimura, A. Inoue, E. Arenholz, and J.-H. Guo, "Temperature and thickness driven spin-reorientation transition in amorphous Co-Fe-Ta-B thin films," *Phys. Rev. B* **73**(5), 052401 (2006).
- <sup>10</sup>P. Sharma, H. Kimura, and A. Inoue, "Tailoring the magnetic properties of mechanically hardest Co-Fe-Ta-B glassy thin films," *J. Appl. Phys.* **101**(9), 09N502 (2007).
- <sup>11</sup>W. Coffey and Y. P. Kalmykov, *The Langevin Equation: With Applications to Stochastic Problems in Physics, Chemistry and Electrical Engineering* (World Scientific, 2012).
- <sup>12</sup>Y. Shimada, M. Shimoda, and O. Kitakami, "Multiple magnetic resonance in amorphous Co-Nb-Zr films with weak perpendicular anisotropy," *Jpn. J. Appl. Phys.* **34**(9R), 4786 (1995).
- <sup>13</sup>F. Schoenstein *et al.*, "Influence of the domain structure on the microwave permeability of soft magnetic films and multilayers," *J. Magn. Magn. Mater.* **292**, 201–209 (2005).
- <sup>14</sup>W. T. Coffey *et al.*, "Effect of an oblique magnetic field on the superparamagnetic relaxation time," *Phys. Rev. B* **52**(22), 15951 (1995).
- <sup>15</sup>W. F. Brown Jr., "Thermal fluctuations of a single-domain particle," *Phys. Rev.* **130**(5), 1677 (1963).
- <sup>16</sup>A. Masood and P. McCloskey, C. Ó. Mathúna, and S. Kulkarni, "Co-based amorphous thin films on silicon with soft magnetic properties," *AIP Adv.* **8**(5), 056109 (2018).
- <sup>17</sup>R. Kubo, M. Toda, and N. Hashitsume, *Statistical Physics II: Nonequilibrium Statistical Mechanics* (Springer Science & Business Media, 2012).
- <sup>18</sup>Y. P. Kalmykov, W. T. Coffey, and S. V. Titov, "Bimodal approximation for anomalous diffusion in a potential," *Phys. Rev. E* **69**(2), 021105 (2004).
- <sup>19</sup>L. Landau and E. Lifshitz, "On the theory of the dispersion of magnetic permeability in ferromagnetic bodies," in *Perspectives in Theoretical Physics* (Elsevier, 1992), pp. 51–65.
- <sup>20</sup>D. Garanin, V. Ishchenko, and L. Panina, "Dynamics of an ensemble of single-domain magnetic particles," *Teor. Mat. Fiz.* **82**(2), 242–256 (1990), available at <https://link.springer.com/content/pdf/10.1007/BF01079045.pdf>.
- <sup>21</sup>Y. L. Raikher and V. I. Stepanov, "Intrinsic magnetic resonance in superparamagnetic systems," *Phys. Rev. B* **51**(22), 16428 (1995).
- <sup>22</sup>I. Klik, "Rotation of magnetization in unison and Langevin equations for a large spin," *J. Stat. Phys.* **66**(1–2), 635–645 (1992).
- <sup>23</sup>W. Coffey, D. Crothers, Y. P. Kalmykov, and S. Titov, "Precessional effects in the linear dynamic susceptibility of uniaxial superparamagnets: Dependence of the ac response on the dissipation parameter," *Phys. Rev. B* **64**(1), 012411 (2001).
- <sup>24</sup>H. Fukushima, Y. Uesaka, Y. Nakatani, and N. Hayashi, "Switching times of a single-domain particle in a field inclined off the easy axis," *J. Appl. Phys.* **101**(1), 013901 (2007).
- <sup>25</sup>L. Geoghegan, W. Coffey, and B. Mulligan, "Differential recurrence relations for non-axially symmetric rotational Fokker-Planck equations," *Adv. Chem. Phys.* **100**, 475–641 (1997).
- <sup>26</sup>M. Yamaguchi *et al.*, "Magnetic thin-film inductors for RF-integrated circuits," *J. Magn. Magn. Mater.* **215**, 807–810 (2000).